2824 *Macromolecules* **2010**, *43*, 2824–2831
DOI: 10.1021/ma9023679

Macromolecules
ARTICLE

Photodegradable Hydrogels to Generate Positive and Negative Features over Multiple Length Scales

Darice Y. Wong,[†] Donald R. Griffin,[‡] Jason Reed,[§] and Andrea M. Kasko*[,†,‡,§]

[†]*Department of Bioengineering, and* [‡]*UCLA Biomedical Engineering IDP, University of California, Los Angeles, California 90095-1600, and* [§]*California Nanosystems Institute, 570 Westwood Plaza, Los Angeles, California 90095*

Received October 23, 2009; Revised Manuscript Received January 25, 2010

ABSTRACT: Here we present a photodegradable hydrogel as a biocompatible, nonfouling photoresist capable of presenting positive and negative features through single-photon and two-photon degradation. An *ortho*-nitrobenzylether (*o*-NBE) moiety is used as a polymerizable cap for poly(ethylene glycol) chains to create a photodegradable macromer. Positive and negative features can be patterned into/onto a hydrogel over a broad range of length scales ($\sim 10^{-7}$ to 10^{-2} m (nm−cm)) in single- and two-photon photolysis. Phase contrast micrographs and profilometry data show that a partially degradable hydrogel network undergoes swelling to produce positive features with varying size (10−100 μm). Conjugation of a coumarin fluorophore to the *o*-NBE macromer enhances the sensitivity of the hydrogel to two-photon degradation, simultaneously incorporating fluorescence visualization with no added dye.

Introduction

Photolithography is a useful patterning tool that uses light to create a discrete pattern in a chemical photoresist. A negative photoresist becomes less soluble when exposed to light, allowing the opaque pattern of the photomask to be rinsed away as a negative feature. A positive photoresist becomes more soluble when exposed to light, allowing the pattern of the photomask to remain as a positive feature (Figure 1). Negative resist materials often consist of small molecule monomers that can be cytotoxic and are thus poorly suited for formation in the presence of live cells. A few researchers have attempted to improve the biocompatibility of current photoresists with limited success. For example, SU-8 2000, a common epoxy-based negative tone photoresist, shows increased primary neuron survival if pretreated with a combination of parylene coating, heat, and sonication.[1] Because of their lack of compatibility, small-molecule negative photoresists are usually formed in the absence of cells and may incorporate cells into/onto the resist postfabrication. In contrast, macromers such as poly(ethylene glycol) (PEG) diacrylate are biocompatible negative tone photoresists. Many examples of biocompatible macromer negative tone photoresists have been reported, including those sensitive to both single-[2,3] and two-photon polymerization.[4,5]

Photodegradable materials, which are positive tone resists, composed of polymer networks have been reported by several groups. In one approach, coumarin groups were attached to the ends of a macromer and dimerized at 365 nm.[6] The dimerization process is reversible, with degradation occurring at 254 nm. In another example, anthracene was attached to multiarmed star PEG and dimerized at 365 nm, with the reversible degradation occurring at 254 nm.[7] Reversible dimerization of cinnamate groups has also been used to stabilize nanostructures formed from PEG-block-poly(L-lactide).[8] In all of these cases, polymerization or dimerization occurs at a cell-compatible wavelength (365 nm), but the wavelength at which degradation occurs, 254 nm, is unsuitable for cells.[9] Johnson et al. reported the synthesis of photodegradable difunctional initiators for ATRP used to produce photocleavable poly(*t*-butyl acrylate).[10] In this example, degradation is cell-compatible, but network formation is not. In a later example, polymer network formation was accomplished using copper-free click chemistry to (theoretically) improve the cytocompatibility, but this system was not used in the presence of live cells.[11]

To date, only one example of a positive hydrogel photoresist has been reported with demonstrated compatibility with live cells.[12,13] These networks (formed from PEG macromers containing *o*-NBE linkers) were chemically and physically patterned on the microscale using single- and two-photon phototolysis, including single-photon photolysis in the presence of live cells. This photodegradable hydrogel platform (which is also the material investigated in this article) has garnered significant attention from the biomaterials and tissue engineering community, as indicated by three spotlight articles[14−16] highlighting the importance of this work. With the increasing activity and sophistication in biotechnology research, scientists are searching for biocompatible materials with more flexibility in design and control, particularly with regard to photoresists. In this work, we further characterize the limits of this hydrogel platform in single- and two-photon photolysis.

Two-photon excitation has been used for 3D lithography in both biological and nonbiological systems. Whereas *o*-NBE moieties are susceptible to two-photon degradation,[12,13] their two-photon absorption cross-section is very low[17] (at $\lambda = 740$ nm, $\delta_u = 0.01$ to 0.03 *GM*). For a two-photon process to be useful in a living biological system, the absorption cross-section should be in the range of 0.3 *GM* or greater,[18] which is significantly higher than that of the *o*-NBE moieties. The *o*-NBE group can be modified to degrade via multiphoton photolysis by coupling it to a coumarin fluorophore.[18] Small-molecule analogs of *o*-NBE moieties conjugated to chloro- or bromo-coumarins have uncaging

*To whom correspondence should be addressed. Address: Department of Bioengineering, 410 Westwood Plaza Engineering V, room 5121H, University of California, Los Angeles, CA 90095-1600. E-mail: akasko@ucla.edu.

 Published on Web 02/24/2010

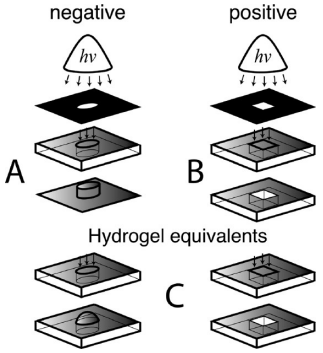

Figure 1. (a) Negative tone and (b) positive tone are exposed to light through a photomask. (c) A single hydrogel can be used to create both raised and pitted features depending on the amount of degradation and the cross-linking density.

cross sections orders of magnitude higher (at $\lambda = 740$ nm, $\delta_u = 0.4$ to 0.7 *GM*) than *o*-NBE moieties alone.[19] Mechanistic studies of 1-(2-nitrophenyl)ethyl)-caged coumarins show rapid photolysis and up to an 800 fold increase in fluorescence after uncaging, also making them ideal candidates for imaging.[19]

Here we report the lithographic capabilities and limitations of a biocompatible hydrogel containing *o*-NBE moieties. Using single- and two-photon photolysis, we can create well-defined positive and negative features over multiple length scales ($\sim 10^{-7}m$ to $10^{-2}m$) in 2D and 3D. We characterize the sensitivity of this macromer to two-photon photolysis at multiple wavelengths (730−872 nm). We also report a new photodegradable macromer containing a coumarin fluorophore to enhance the sensitivity of a hydrogel to two-photon photolysis and compare it with the photodegradable *o*-NBE macromer.

Experimental Section

Materials. Acryloyl chloride (AC) (Alfa Aesar, 96%), triethylamine (TEA) (Fisher Scientific, 99%), ammonium persulfate (AP) (J.T. Baker, 98%), tetramethylethylenediamine (TEMED) (EMD, 99%), tetrahydrofuran (THF) (Fisher Scientific, 99.9%), chloroform (Fisher Scientific, 99.9%), phosphorus pentachloride (Alfa Aesar, 98%), sulfuric acid (EMD, 50%), sodium hypochlorite (Fisher Scientific, 6%), piperidine (Spectrum Chemical MFG. Corp., 99%), malonic acid (Alfa Aesar, 99%), pyridine (Fisher Scientific, 99.9%), aniline (Sigma Aldrich, 99.5%), ethanol (Pharmco-AAPER, 99.5%), 2-hydroxyethyl methacrylate (Sigma Aldrich, 97%), dichloromethane (DCM) (Fisher Scientific, 99.9%), acetone (Fisher Scientific, 99.7%), potassium carbonate (Sigma Aldrich, 99%), sodium iodide (EM Science, 99.5%), magnesium sulfate (Fisher Scientific, 99.6%), 2,4-dihydroxy benzldehyde (Acros Organics, 98%), *N*,*N*-dimethylformamide (DMF) (Fisher Scientific, 99.8%), poly(ethylene glycol) (PEG) ($M_n = 4000$ g/mol) (Mallinckrodt Chemicals), and diethyl ether (Fisher Scientific, 99.9%) were used as received unless otherwise noted. AC was distilled under vacuum into an airfree flask and stored under a blanket of Ar at −20 °C in the absence of light. TEA was distilled under Ar and stored over KOH pellets. THF was distilled from CaH_2 and stored under Ar in a dry, air-free flask. DCM was distilled and stored under Ar in a dry, airfree flask. DMF was stored over activated type 4A molecular sieves. PEG 4000 diacrylate was synthesized according to a modified literature procedure.[20] 4-(4-(1-Hydroxyethyl)-2-methoxy-5-nitrophenoxy)butanoic acid was synthesized according to a modified literature procedure.[12]

Techniques. All reactions were performed under a N_2 atmosphere using a Schlenk line unless otherwise noted. ^{1}H NMR spectra (δ) were recorded on a Bruker Biospin Ultrashield 300 MHz NMR spectrometer. Unless otherwise noted, all spectra were recorded in $(CD_3)_2SO$ or $CDCl_3$ using TMS as an internal standard.

Synthesis. *4-(4-(1-(Acryloyloxy)ethyl)-2-methoxy-5-nitrophenoxy)butanoic Acid.* 4-(4-(1-Hydroxyethyl)-2-methoxy-5-nitrophenoxy)butanoic acid (4.53 g, 15.1 mmol) and TEA (8.28 mL, 59.4 mmol) were dissolved in a solution of THF (50 mL) and cooled to 0 °C. To this solution, a mixture of AC (2.82 mL, 52.0 mmol) and THF (10 mL) was added dropwise. The reaction mixture was stirred 24 h and monitored by ^{1}H NMR. Upon completion, the reaction mixture was poured in water (1.2 L), stirred at room temperature for 2 h, extracted with chloroform (5 × 200 mL), dried over $MgSO_4$, and concentrated to dryness via rotary evaporation to yield 5.26 g (98%) as a viscous yellow liquid. ^{1}H NMR ($CDCl_3$, δ): 7.60 (s, Ar-**H** *ortho* to Ar-NO_2), 7.02 (s, Ar-**H** *meta* to Ar-NO_2), 6.55 (m, Ar-C**H**(CH_3)OCHCH$_2$), 6.42, 5.85 (d, d, Ar-OCHCHC**H**$_2$), 6.16 (m, Ar-OCHC**H**CH$_2$), 4.10 (t, Ar-OC**H**$_2$CH$_2$CH$_2$CO$_2$H), 3.92 (s, Ar-OC**H**$_3$), 2.58 (t, Ar-OCH$_2$CH$_2$C**H**$_2$CO$_2$H), 2.23 (m, Ar-OCH$_2$C**H**$_2$CH$_2$CO$_2$H), 1.65 (d, Ar-CHC**H**$_3$).

Bis(4-(4-(1-(acryloyloxy)ethyl)-2-methoxy-5-nitrophenoxy)-butanate)PEG (M_n = *4668*) (*Photodegradable Macromer*). 4-(4-(1-(Acryloyloxy)ethyl)-2-methoxy-5-nitrophenoxy)butanoic acid (5.26 g, 14.89 mmol) was reacted with phosphorus pentachloride (3.26 g, 8.9 mmol) for 30 min at RT. The resultant phosphorus oxychloride was removed under reduced pressure, and the residue was dissolved in DCM (40 mL). The solution was added dropwise to a solution of PEG (14.89 g, 3.7 mmol) and TEA (2.08 mL, 14.9 mmol) in DCM (50 mL). After stirring 20 h at RT, the reaction was filtered and evaporated via rotary evaporation. The residue was dissolved in acetone (50 mL), and the TEA salts were removed by filtration. The product was collected by precipitation in diethyl ether (750 mL) at −20 °C and filtration to obtain a very pale-yellow powder (14.20 g, 81.7%). ^{1}H NMR ($CDCl_3$, δ): 7.60 (s, Ar-**H** *ortho* to Ar-NO_2), 7.02 (s, Ar-**H** *meta* to Ar-NO_2), 6.55 (m, Ar-C**H**(CH_3)-OCHCH$_2$), 6.42, 5.85 (d, d, Ar-OCHCHC**H**$_2$), 6.16 (m, Ar-OCHC**H**CH$_2$), 4.25 (t, Ar-OCH$_2$CH$_2$CH$_2$CO$_2$C**H**$_2$), 4.10 (t, Ar-OC**H**$_2$CH$_2$CH$_2$CO$_2$R), 3.92 (s, Ar-OC**H**$_3$), 3.56−3.75 (m, 347-H[1]), 2.58 (t, Ar OCH$_2$CH$_2$C**H**$_2$CO$_2$R), 2.17 (m, Ar OCH$_2$C**H**$_2$CH$_2$CO$_2$R), 1.65 (d, Ar-CHC**H**$_3$).

1-(5-Chloro-2,4-dihydroxyphenyl)ethanone. 2,4-Dihydroxy benzaldehyde (5.00 g, 36.2 mmol) was dissolved at room temperature in a solution of sulfuric acid (55 mL) and water (55 mL) and then cooled to 0 °C. Piperidine (3.60 g, 42.3 mmol) was added dropwise to a solution of aqueous sodium hypochlorite (55 mL, 41.4 mmol) at 0 °C and then added dropwise to the aqueous sulfuric acid mixture and stirred for 20 h. The chlorinated product was collected by filtration and washed with water to yield 3.75 g (60.0%) as a yellow powder. The product was a 1:2 mixture of 3- and 5-chloro isomers and was used without further purification. (Reported yield represents only 5-chloro-isomer) ^{1}H NMR ($(CD_3)_2SO$, δ): 10.89 (s, Ar-O**H**), 9.93 (s, Ar-C**H**O), 7.57 (s, Ar-**H** *ortho* to Ar-Cl), 6.54 (s, Ar-**H** *meta* to Ar-Cl).

6-Chloro-7-hydroxycoumarin-3-carboxylate (*Coumarin*). 1-(5-Chloro-2,4-dihydroxyphenyl)ethanone (3.75 g, 21.7 mmol)) was combined with malonic acid (6.44 g, 65.2 mmol), aniline (catalytic), and pyridine (25 mL). After stirring for 2 days, the reaction was quenched in ethanol (80 mL), filtered, and washed with aqueous hydrochloric acid (0.1 N, 5 × 50 mL), H_2O (3 × 50 mL) and diethyl ether (2 × 50 mL). The resultant powder was dried under vacuum (2.98 g, 57%) (note, no product due to 3-chloro is detected). ^{1}H NMR ($(CD_3)_2SO$, δ): 13.00 (s, −COO**H**), 11.94 (s, O**H**), 8.64 (s), 7.98 (s), 6.87 (s).

2-(Methacryloyloxy)ethyl 6-Chloro-7-hydroxycoumarin-3-carboxylate (*Coumarin-HEMA Conjugate*). 6-Chloro-7-hydroxy-2-oxo-2H-chromene-3-carboxylic acid (coumarin) (0.50 g, 2.1 mmol) was reacted with phosphorus pentachloride (0.45 g, 4.2 mmol) for 30 min at RT. The resultant phosphorus oxychloride was removed under reduced pressure, and the residue was dissolved in DCM (3 mL). The solution was added dropwise

to a solution of 2-hydroxyethyl methacrylate (0.25 g, 1.9 mmol) and TEA (0.52 mL, 3.7 mmol) in DCM (20 mL). After stirring 20 h at RT, the reaction was filtered and evaporated via rotary evaporation. The residue was dissolved in acetone (5 mL), and the TEA salts were removed by filtration; subsequently, the solution was passed through a silica plug. After acetone was removed by rotary evaporation, the residue was dissolved in DCM (5 mL) and dried over $MgSO_4$. $MgSO_4$ was removed by filtration, and the product was collected by rotary evaporation to obtain a dark-brown residue (0.57 g, 87%). ^{1}H NMR ($(CD_3)_2SO$, δ): 8.65 (s, 1H), 8.02 (s, 1H), 7.65 (s, 1H), 6.04, 5.64 (s, $C(CH_3)CH_2$), 4.45 (t, $COOCH_2CH_2$), 4.35 (t, $COOCH_2CH_2$), 1.84 (s, $C(CH_3)CH_2$).

Bis(4-(4-(1-chloroethyl)-2-methoxy-5-nitrophenoxy)butanate) PEG (M_n = 4600) (Chlorinated Photodegradable Macromer). 4-(4-(1-Hydroxyethyl)-2-methoxy-5-nitrophenoxy)butanoic acid (0.5 g, 1.7 mmol) was reacted with phosphorus pentachloride (0.72 g, 3.4 mmol) for 30 min at RT. The resultant phosphorus oxychloride was removed under reduced pressure, and the residue was dissolved in DCM (10 mL). Added dropwise to this solution was a solution of PEG (1.90 g, 0.5 mmol) and TEA (0.27 mL, 1.9 mmol) in DCM (20 mL). After stirring 20 h at RT, the reaction was filtered and evaporated via rotary evaporation. The residue was dissolved in acetone (10 mL), and the TEA salts were removed by filtration. The product was collected by precipitation in diethyl ether (350 mL) at −20 °C and filtration to obtain a very pale-yellow powder (1.90 g, 85%). ^{1}H NMR ($CDCl_3$, δ): 7.45 (s, Ar-**H** *ortho* to Ar-NO_2), 7.27 (s, Ar-**H** *meta* to Ar-NO_2), 5.89 (m, Ar-C**H**Cl), 4.22 (t, Ar-$OCH_2CH_2CH_2CO_2CH_2$), 4.10 (t, Ar-$OCH_2CH_2CH_2CO_2$R), 3.95 (s, Ar-OCH_3), 3.49−3.70 (m, 347-H^1), 2.55 (t, Ar $OCH_2CH_2CH_2CO_2$R), 2.12 (m, Ar $OCH_2CH_2CH_2CO_2$R), 1.83 (d, Ar-$CHCH_3$).

Bis(4-(4-(1-((2-(methacryloyloxy)ethyl 6-Chloro-7-hydroxy-coumarin-3-carboxyl)oxy)ethyl)-2-methoxy-5-nitrophenoxy)butanate) PEG (M_n = 5236) (Coumarin-Conjugate Macromer). The chlorinated photodegradable macromer, bis(4-(4-(1-chloroethyl)-2-methoxy-5-nitrophenoxy)butanate) PEG (M_n = 4600) (1.07 g, 0.2 mmol), was dissolved in DMF (10 mL) and stirred with NaI (66 mg, 0.4 mmol). Potassium carbonate (0.10 g, 0.7 mmol) and the coumarin-HEMA conjugate, 2-(methacryloyloxy)ethyl 6-chloro-7-hydroxy-2-oxo-2*H*-chromene-3-carboxylate (0.20 g, 0.6 mmol), were dissolved in DMF (10 mL). All solutions were combined and heated to 100 °C for 9 days. The product was precipitated in diethyl ether (350 mL) at −20 °C. The residue was dissolved in DCM (5 mL) and dried with $MgSO_4$. The $MgSO_4$ was removed by filtration, and the product was collected by rotary evaporation (0.69 g, 66.5% yield, 60% chloro substitution). ^{1}H NMR ($CDCl_3$, δ): 8.38 (s, 1H), 7.57 (s, 1H), 7.55 (s, Ar-**H** *ortho* to Ar-NO_2), 7.33 (s, Ar-**H** *meta* to Ar-NO_2), 6.99 (s, 1H), 6.14, 6.58 (s, $C(CH_3)CH_2$), 5.56 (m, Ar-C**H**OR), 4.55 (t, $COOCH_2CH_2$), 4.45 (t, $COOCH_2CH_2$), 4.25 (t, Ar-$OCH_2CH_2CH_2CO_2CH_2$), 4.12 (t, Ar-$OCH_2CH_2CH_2CO_2$R), 3.97 (s, Ar-OCH_3), 3.54−3.73 (m, 347-H^1), 2.57 (t, Ar-$OCH_2CH_2CH_2CO_2$R), 2.16 (m, Ar-$OCH_2CH_2CH_2CO_2$R), 1.95 (s, $C(CH_3)CH_2$), 1.55 (d, Ar-$CHCH_3$).

Hydrogel Fabrication. To distinguish between the different gels used in this report, we will use the following terminology: gels formed from the photodegradable macromer in Scheme 1 will be called "*o*-NBE gels"; gels formed from the coumarin-conjugate macromer in Scheme 4 will be called "coumarin-*o*-NBE gels"; and gels fabricated using the photodegradable macromer in Scheme 1 and poly(ethylene glycol) diacrylate will be referred to as "partially degradable gels".

All hydrogels were fabricated by dissolving PEG 4000 diacrylate, the photodegradable macromer, or the coumarin-conjugate macromer in water at different wt % depending on the experiment. Solutions of APS (20 wt % in water) and TEMED (5% by volume in water) were used to radically polymerize the macromers at final concentrations of 0.05 M APS and 0.025 M

Scheme 1. Synthesis of Bis(4-(4-(1-(acryloyloxy)ethyl)-2-methoxy-5-nitrophenoxy)butanate) PEG (M_n = 4668) (Photodegradable Macromer)

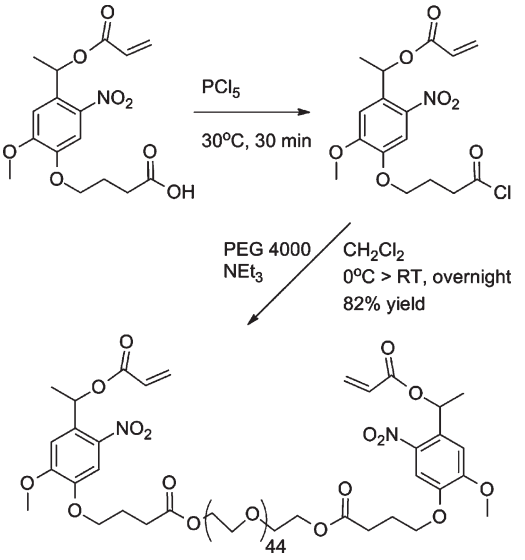

TEMED. The mixtures were vortexed and quickly dispersed between two glass microscope slides with 0.55 mm spacers. Photodegradable macromer, when used alone, was polymerized at 20 wt % to form the "*o*-NBE gel". A mixture of PEG 4000 diacrylate and the coumarin-conjugate macromer was polymerized using 20 wt % PEG and 1 wt % coumarin-conjugate macromer to form the "coumarin-*o*-NBE gel". A mixture of the photodegradable macromer and PEG 4000 diacrylate was polymerized using 10 wt % PEG and 10 wt % photodegradable macromer to create the "partially degradable gel". Thin films of hydrogel were cast by capillary action using aluminum foil as spacers between a glass slide and silicon substrate. Two different compositions were used: (1) 20 wt % photodegradable macromer and (2) 10 wt % photodegradable macromer and 10 wt % PEG 4000 diacrylate.

Microscopy. All confocal and two-photon microscopy images and experiments were performed in the Advanced Light Microscopy/Spectroscopy laboratory at California Nanosystems Institute (CNSI) at UCLA. Typical phase contrast micrographs were obtained using a Zeiss Axiovert Observer Z1 inverted fluorescent microscope. Profilometry was performed on a Veeco NT 9300 Optical Profiler in the Nano & Pico Characterization Laboratory at CNSI, UCLA.

Patterned Degradation of Hydrogels. *Single-Photon Degradation.* Photomasks were placed directly onto hydrogel surfaces. An Omnicure 1000 mercury vapor lamp (EXFO) equipped with a 365 nm narrow bandpass filter was used to deliver ultraviolet light (10−20 mW/cm^2) for times ranging from 1 to 30 min to achieve surface etching through the photomask. Light intensity was measured with a UVX digital radiometer (UVP). Topographic features were examined by phase contrast microscopy and interferometric profilometry. For samples examined by profilometry, the Omnicure lamp with 365 nm filter was used to degrade both thin film gels through a photomask of 100 μm squares. The power delivered to each hydrogel during degradation was 18.5 mW/cm^2 for 5 min each. Degraded surface topographies were analyzed using an interferometric microscope.

Two-Photon Degradation. Hydrogels were cast between glass slides and then replaced with no. 1 glass coverslips. Moisture was maintained by the addition of water. A Leica Confocal CTR MIC microscope was used to create specific designed voids within hydrogels. Regions of interest were drawn within the Leica Confocal Software for scanning using the multiphoton laser (Spectra-Physics NESLAB KMC 100, Maitai Pulsing

Scheme 2. Synthesis of 6-Chloro-7-hydroxycoumarin-3-carboxylate (Coumarin)

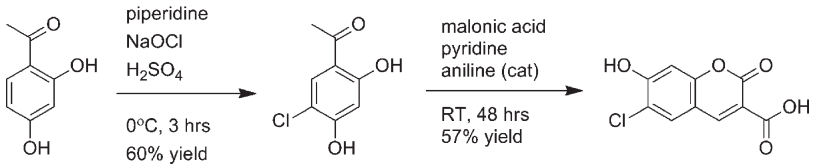

laser, Thermo Elecron Corp.) at 1.5 to 1.8 W. A 40× oil immersion objective (NA = 1.25) was used at a zoom factor of 5 for degradative scans. The same lens was used at zoom factor 1 for a single scan to obtain fluorescent images of the coumarin-*o*-NBE gel immediately after degradative scans. For *z*-stack confocal images, step size was 1 μm and pinhole size was set to 600 μm. The number of scans and wavelength were varied, with wavelengths from 872 to 730 nm.

Results and Discussion

Macromer Synthesis. Although the photodegradable macromer containing *o*-NBE has already been reported,[12] we have slightly modified the conjugation of acrylated *o*-NBE group to poly(ethylene glycol) (PEG). Instead of using bis-amine end-functionalized PEG (which is significantly more expensive) to form an amide linkage via peptide coupling chemistry, we convert the *o*-NBE to an acid chloride and directly esterify PEG in high yield (Scheme 1). The ester conjugation is more efficient and easier to purify. Whereas the ester linkage is more susceptible to hydrolysis than the original amide, this degradation is so slow that PEG hydrogels containing this ester linkage are commonly modified with lactide/glycolide repeat units to impart hydrolytic instability. The ester linkage does not significantly change the functionality or stability of hydrogels, as demonstrated in these studies. For experiments such as the ones presented here and other future uses on short time scales (a few months), production by ester conjugation is preferable.

To obtain a macromer with improved sensitivity to two-photon degradation, we conjugated a coumarin fluorophore directly to the *o*-NBE group. 6-Chloro-7-hydroxycoumarin (coumarin) was synthesized by first chlorinating 2,4-dihydroxybenazdehyde using a mixture of piperidine and bleach in sulfuric acid. Both the 3-chloro and 5-chloro isomers are formed, but the product is used without purification; the 3-chloro isomer is unreactive in the condensation with malonic acid, and only the desired product is obtained (Scheme 2). The resulting 6-chloro-7-hydroxycoumarin is converted to the acid chloride and used to esterify hydroxy ethyl methacrylate (Scheme S1 of the Supporting Information). This coumarin monomer is then used to etherify the benzyl chloride positions of bis(4-(4-(1-chloroethyl)-2-methoxy-5-nitrophenoxy)butanoyl PEG (Scheme 3) to produce the coumarin-conjugate macromer (Scheme 4).

Photodegradable hydrogels are fabricated via free-radical polymerization of these macromers in water using APS/TEMED to produce initiating radicals. Gelation is rapid ($<10 \sim 20$ min) and can be controlled by varying the concentration of APS/TEMED. The gels are colorless to slightly yellow and optically clear.

Both single- and multiphoton degradation can control the hydrogel network properties over a broad range of length scales (nanoscale to macroscale). The smallest feature size that can be produced by a Gaussian laser beam with diameter, *D*, and a depth of focus, *L*, at a given numerical aperture (*NA*) is related to the wavelength

Scheme 3. Synthesis of Bis(4-(4-(1-chloroethyl)-2-methoxy-5-nitrophenoxy)butanate) PEG (M_n = 4600) (Chlorinated Photodegradable Macromer)

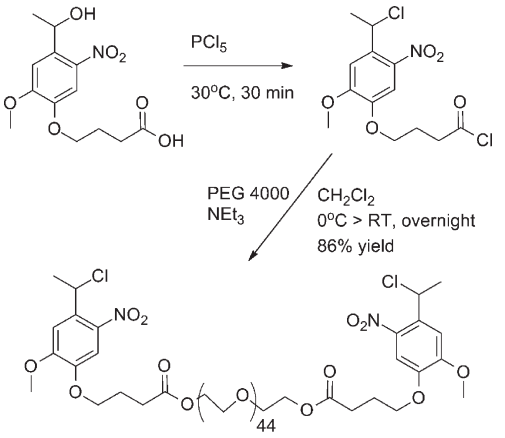

of light and *m*:

$$D_{\mathrm{FWHM}} = \frac{2}{\pi NA}\sqrt{\frac{\ln 2}{2m}} \quad (1)$$

$$L_{\mathrm{FWHM}} = \frac{2}{\pi NA^2}\sqrt{2^{1/m}-1} \quad (2)$$

For two-photon photolysis, $m = 2$ and $\lambda = 730$ nm, so $D = 154$ nm and $L = 191$ nm (using $NA = 1.25$, representative of the experiments in this article). In single-photon photolysis, $m = 1$ and degradation occurs at $\lambda = 365$ nm, so $D = 137$ nm and $L = 232$ nm (using $NA = 1$). The theoretical limits of resolution are estimated to be a few hundred nanometers in diameter as well as focal depth for both single- and two-photon activation. Combined with these limits, the photolytic capabilities of this hydrogel system present an unprecedented level of spatial control over hydrogel scaffold structure and chemistry.

Formation of Negative Features. 20 wt % *o*-NBE gels were exposed to 365 nm light to create macro- and microsurface features via single-photon degradation (Figure 2).

Surface erosion and through-gel lithography were previously demonstrated to form features on the order of 10^{-4} m.[12] Arbitrary features (determined only by the pattern of the photomask) are created rapidly ($t < 10$ min) using cell-compatible wavelengths and intensities. Macroscopic patterns visible to the naked eye are easily created, and features on the order of 10^{-5} m are also accessible (Figure 2). Although nanoscale features are possible in both single- and two-photon degradation, commercial photomask printing technology limits resolution to $\sim$10 μm.

Formation of Positive Features. The volumetric swelling ratio (*Q*) of a hydrogel scales inversely with the cross-link density (ρ_x) according to eq 3. Partial photodegradation in a local area will result in decreased cross-link density and

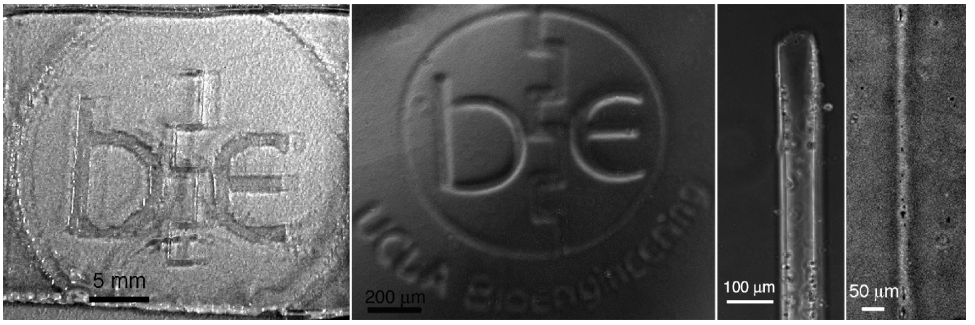

Figure 2. Features are degraded into the surface of hydrogels on multiple length scales. Left to right: 3 cm diameter design is visibly degraded into the hydrogel. A similar design is degraded into the surface on the several hundred micrometers scale. Lines of 100 and 30 μm are degraded into the surface, verifiable by the debris collected in the wells.

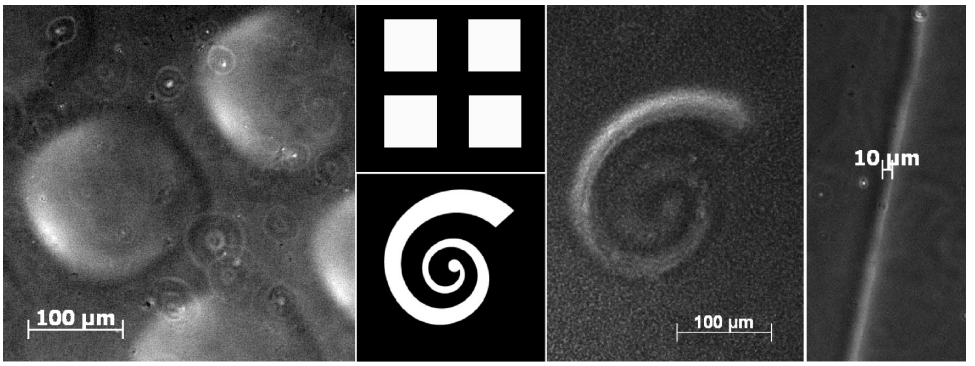

Figure 3. Raised features are created by partially degrading the surface of hydrogels on multiple length scales. Left to right: 100 μm squares appear as rounded protrusions in contrast with the mask used to create them (center top). Raised spirals display a smaller feature size in the line. A 10 μm line appears as a raised ridge.

Scheme 4. Synthesis of Bis(4-(4-(1-((2-(methacryloyloxy)ethyl 6-Chloro-7-hydroxycoumarin-3-carboxyl)oxy)ethyl)-2-methoxy-5-nitrophenoxy)butanate) PEG (M_n = 5236) (Coumarin-Conjugate Macromer)

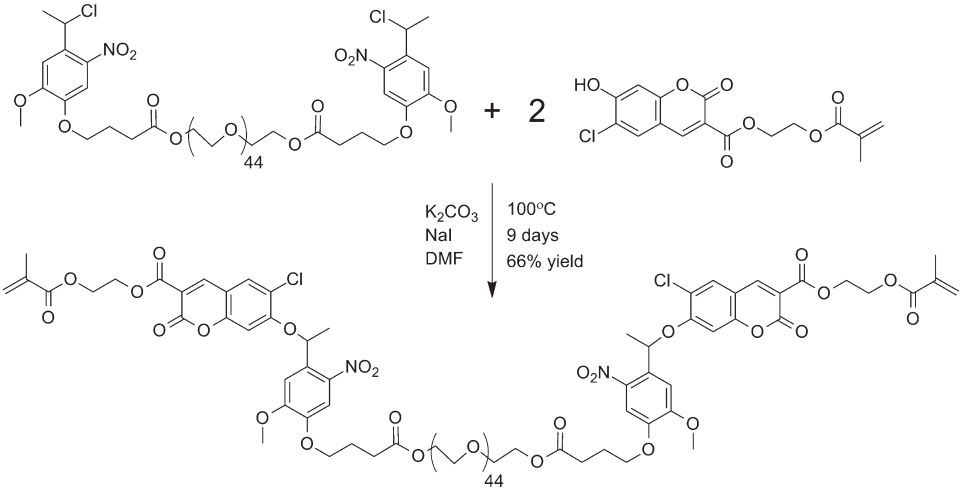

increased swelling, providing a means to etch soft positive features onto a hydrogel. In a gel in which 50% of the cross-links degrade, such as the partially degradable gels in Figure 3, we can expect a maximum increase in the volume of the degraded portion of 52% (eq 4). If the system is spatially confined in two dimensions, like the thin films analyzed in Figure 4, then the maximum feature height is related to the excess volume (although polymer chain elasticity should constrain the feature to a somewhat smaller volume). The formed features should also have a decreased elastic modulus (~15% softer if 50% of the cross-links degrade, eq 5), potentially making them quite fragile.

$$Q \propto \rho_x^{-3/5} \tag{3}$$

$$\frac{Q}{Q_0} = \left(\frac{\rho_x}{\rho_{x0}}\right)^{-3/5} \tag{4}$$

$$E \propto \rho_x^{6/5} \tag{5}$$

All Gels Creating Positive Features Were Partially Degradable. To obtain positive features, we exposed hydrogels to

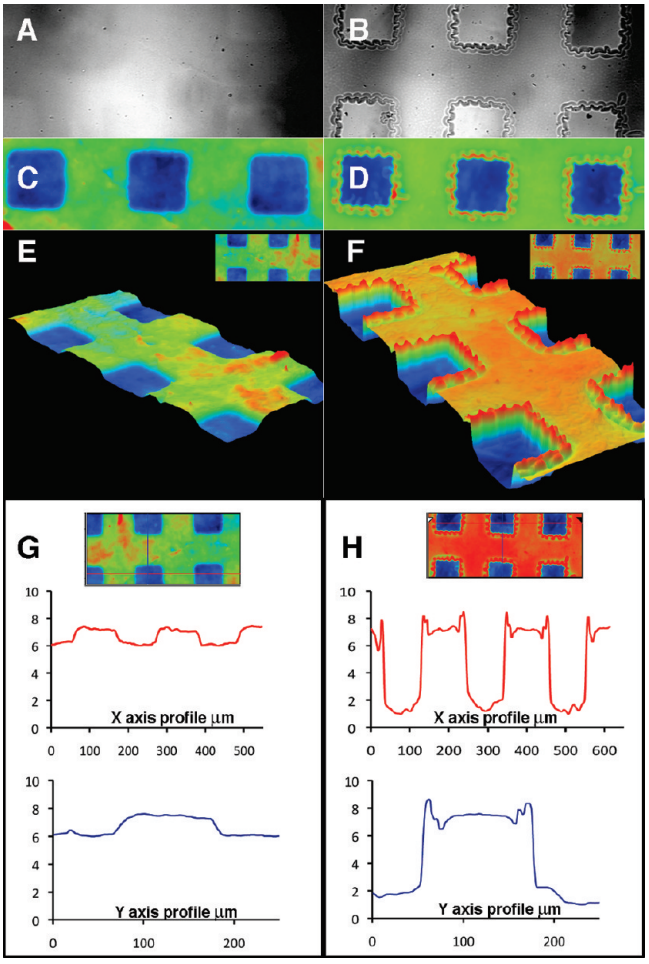

Figure 4. Brightfield microscope images of (a) fully degradable *o*-NBE gel and (b) partially degradable *o*-NBE gel as thin films on a silicon substrate. (c,d) Top view of the optical thickness images for those gels. (e,f) 3D rotation shows the profiles for the degraded surfaces rendered from the optical thickness. (g,h) Horizontal and vertical cross-sectional thickness are plotted to show the range of heights for both gels (axes are micrometers).

intermittent amounts of light (complete degradation occurs in ~10 min) to obtain partial degradation. Positive feature formation can be seen in Figure 3, where a hydrogel containing *o*-NBE macromer was exposed through a photomask (100 μm squares, spirals, or 10 μm line) for 4 min; after the gel was allowed to reach equilibrium swelling, it was imaged using phase contrast microscopy. Although the patterns transfer well to the hydrogel substrate, the features are slightly larger than the feature size of the photomask, which may be a result of scattered light in addition to swelling. Whereas the square-pattern photomask contains sharp corners, these corners are blunted upon transfer to the hydrogel because of the elastic nature of the substrate. In contrast, the spiral pattern, which contains no corners or notches to concentrate the stress, is not distorted.

To confirm the formation of positive features seen in the phase contrast micrographs, we characterized fully and partially degradable hydrogels using profilometry with an interferometric microscope based on a modified Veeco NT 9300 Optical Profiler.5. This instrument can measure the relative height of reflective objects in the field of view to better than 1 nm precision under ideal conditions in various liquids. It can also quantify the phase shift imparted on light reflected from the substrate caused by propagation through transparent objects immersed in liquid. This phase shift is proportional to material density at each pixel and is called optical thickness. Optical thickness determined by interferometry is a well-established technique to measure quantitatively and noninvasively local material density in transparent samples.[21] The optical thickness of the gel can be converted to physical height by measuring the distance between the substrate and reflective microspheres on the surface of the gel, using vertical scanning interferometry. This method is described in detail elsewhere.[22] Here we interrogated several points across each of the gels to determine an average conversion constant of 0.052 + 0.008 μm per nm optical thickness.

The photodegradable macromer was either homopolymerized to create a fully degradable hydrogel or copolymerized in a 1:1 mixture with PEG diacrylate to create a partially degradable hydrogel. The polymerization mixtures were cast as thin films and allowed to cure. The formation of these thin films is described in the methods**.** Subsequently, these thin films were exposed to 365 nm light through a photomask (100 μm squares) for 5 min each. Analysis of the topography revealed that the films were 7 to 7.5 μm thick. Fully degradable hydrogels produced features 1 to 1.5 μm deep (Figure 4a,c, g,e), confirming the formation of negative features. Partially degradable hydrogels also produce negative features 5 to 5.5 μm deep (Figure 4b,d,f,h). The difference in feature depth is a function of light attenuation, which is proportional to the concentration of *o*-NBE groups. Because the partially photodegradable hydrogel contains a lower concentration of the attenuating group, light penetration is deeper.

Of particular interest, the partially degradable hydrogel shows ruffling at the periphery, with a ruffle height on the order of ~1 μm. No ruffle or raised edge is found in the fully degradable thin film. An increase in the swelling ratio puts increased stress at the interface of the swollen feature and the undegraded portion. The fragility of a thin film allows the increased stress during handling to cause rupture of swollen features. These ruptures and ruffles are not seen in the thicker samples used for phase constrast images, where the feature is less likely to dry out and is not only confined on the edges but also covalently linked to a thick and pliant substrate (further thickness of the hydrogel) in contrast with the thin film. The ruffled edges are direct evidence of this swelling and rupture, and, in combination with the phase contrast microscopy images, indicate that positive features are forming. Whereas ideally, the swelling height measurement would be made in the original samples created (Figure 3), the gel must be a thin film attached to a silicon wafer to make these optical measurements without touching the sample.

Two-Photon Degradation. Despite the low absorptivity of the *o*-NBE group at long wavelengths and the low two-photon absorption cross-section (0.01 to 0.03*GM*), it is easily degraded via two-photon photolysis, as demonstrated previously[12] and in Figure 5. We determined the relative sensitivity of the *o*-NBE hydrogel to three different wavelengths of light used for two-photon photolysis: 730, 810, and 872 nm. These three wavelengths are exactly double the wavelength of three common single-photon degradation wavelengths, 365, 405, and 436 nm, accessible from a mercury vapor lamp. The laser power for these wavelengths was relatively unchanged at 1.54, 1.78, and 1.67, respectively. The *o*-NBE group exhibits a maximum absorptivity near 365 nm, and its absorptivity rapidly decreases with increasing wavelength (Figure S1 of the Supporting Information). At cell compatible intensities and time scales (I_0 < 20 mW/cm^2, t < 30 min), the *o*-NBE group is susceptible to single-photon degradation at 365 and 405 nm[12] and significantly less so at

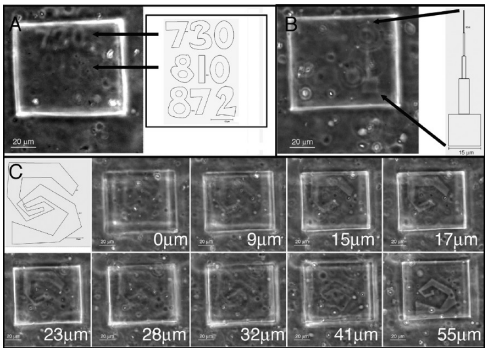

Figure 5. Two-photon degradation of *o*-NBE hydrogel. (a) Wavelengths of light used for degradation were switched among 730, 810, and 872 nm, each for 60 scans. The region of interest outlines are shown. Arrows indicate the 730 and 810 nm wavelength features are visible, whereas 872 nm wavelength exposure did not achieve a visible feature. (b) Lines of decreasing width were degraded at 730 nm for 60 scans. The widths of the rectangles were 15, 5, 2.5, 1, and 0.5 μm. (c) *o*-NBE hydrogel is degraded at different *z* positions as closed voids. Outlines of the two polygonal regions of interest are shown. Advancing focal planes through the degraded area show two separate regions of interest that begin and end separately.

436 nm (unpublished results). Regions of interest were defined to represent the wavelength supplied by the laser for degradation (Figure 5a, right). The photodegradable macromer itself is not fluorescent, and thus network degradation is only visible by phase contrast microscopy. The amount of visible network degradation decreases as wavelength increases (Figure 5a left), showing no visible degradation at 872 nm and the greatest degradation at 730 nm. This correlates well with the single-photon degradation as a function of wavelength at 365−436 nm and confirms that the mechanism for the degradation is truly the excitation of the *o*-NBE group rather than nonspecific scission of random bonds in the network.

Decreasing line widths were created (Figure 5b, right) to demonstrate submicrometer photolithography. Although it may be difficult to see in 2D images, two-photon degradation can be used to etch submicrometer features within the volume of a hydrogel. Feature size is limited by the methods of delivery of excitation (as specified in eqs 1 and 2) and of detection and verification of the features created.

To demonstrate enclosed voids within the *o*-NBE gel, two separate polygons were degraded at different *z* positions, with overlapping sections; that is, whereas the polygons appear to overlap when observing from the top down ($x-y$ direction), they are in completely separate planes in the *z* direction. Figure 5c shows sequential phase contast micrographs of the etched polyhedrons as a function of observation (*z* axis) depth in the hydrogel. The two polygons are visible in separate focal planes and are separated by roughly 40 μm in the *z* direction. This displays the ability to design and execute complex 3D architectures within a biocompatible hydrogel.

To determine the two-photon sensitivity of the hydrogels both with and without the coumarin fluorophore conjugated directly to the *o*-NBE group, we created two sets of hydrogels. The photodegradable macromer was polymerized at 20 wt % in water (*o*-NBE hydrogel); the coumarin-conjugate macromer was polymerized at 1 wt % in water along with 20 wt % PEG diacrylate using the same polymerization conditions. Figure 6a−d demonstrates two-photon degradation of the coumarin-*o*-NBE hydrogel to create arbitrary features on the micrometer scale that are fully contained within the hydrogel. Biologically relevant designs can be

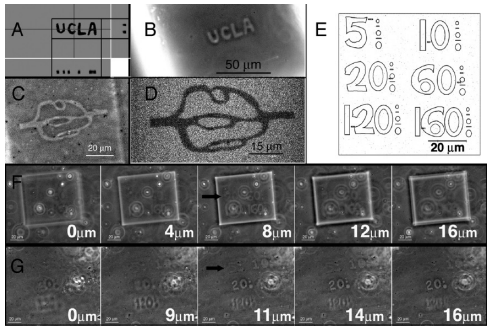

Figure 6. Two-photon degradation of photodegradable hydrogels produce microscale features within the gels. (a) Z-stack confocal scan: Arbitrary designs degraded within minutes in the coumarin-*o*-NBE hydrogel are fully contained within a few micrometers thickness. (b) Phase contrast microscope image confirms the network degradation seen in the confocal fluorescence image. (c) Phase contrast image of a network design containing tapering lines with submicrometer widths. (d) Fluorescent confocal image of coumarin-*o*-NBE gel with network design. (e) Sample region of interest outline used to produce voids of varying thickness correlated to a representative number of scans along with the circles and lines directly adjacent. Sampling of phase images with relative focal depth was taken of the (f) *o*-NBE hydrogel and the (g) coumarin-*o*-NBE hydrogel through similar thicknesses to reveal the relative levels of degradation that occur with different durations of scanning. Arrows indicate the location of the lowest scan number visible: (f) Twenty scans in the *o*-NBE hydrogel and (g) five scans in the coumarin-*o*-NBE hydrogel.

made with thicknesses below 1 μm and imaged with the sensitivity of fluorescent confocal microscopy (Figure 6d). Because of the presence of the coumarin-conjugate as the polymerizing part of the hydrogel network, fluorescent imaging of this type of system can be definitively attributed to true network degradation. This is confirmed with phase contrast microscope images of these same degraded patterns (Figure 6b,c).

To compare the degradation of the hydrogels with and without the coumarin fluorophore, both hydogels were degraded according to the pattern in Figure 6e. Regions of interest were defined in the shapes of numbers to represent the number of scans used to create each region (5, 10, 20, 60, 120, 160 scans), with a single scan corresponding to 1.8 s of exposure, for total exposure times between 9 s and 4.8 min. Figure 6f shows the phase contrast micrographs for the *o*-NBE hydrogel, and Figure 6g shows the phase contrast micrographs for the coumarin-*o*-NBE hydrogel. In the *o*-NBE hydrogel, degradation is only visible after at least 20 scans (36 s exposure), whereas etching of the coumarin-*o*-NBE gel is apparent after only five scans (9 s exposure); the 160 scan feature was not used in the coumarin-*o*-NBE hydrogel. Because the coumarin-*o*-NBE hydrogel can be degraded using fewer scans of equal intensity than the *o*-NBE hydrogel, we can conclude that even this small amount of coumarin-conjugate macromer incorporated in the hydrogel significantly enhances its two-photon photolysis.

Conclusions

We have demonstrated the use of an *ortho*-nitrobenzylether group in a poly(ethylene glycol) hydrogel network to create positive and negative features over a broad range of length scales ($\sim 10^{-7}$ to 10^{-2} m (nm−cm)) using single- and two-photon photolysis. Feature sizes are limited only by the theoretical limits of diffraction under various methods of illumination or activation by light. Additionally, a new coumarin conjugate of the photodegradable macromer has increased sensitivity to

two-photon degradation as well as the ability to be imaged fluorescently. This photodegradable hydrogel system has the potential to fill an increasing need for versatile, biocompatible photolabile materials in a wide range of biotechnology applications.

Acknowledgment. Research support was provided by the UCLA Henry Samueli School of Engineering and Applied Science Start-up Funds.

Supporting Information Available: Schemes for synthesis of 4-(4-(1-(acryloyloxy)ethyl)-2-methoxy-5-nitrophenoxy)butanoic acid and 2-(methacryloyloxy)ethyl 6-chloro-7-hydroxycoumarin-3-carboxylate (coumarin-HEMA conjugate) and absorption spectra of coumarin-conjugate macromer and *o*-NBE monomer (4-(4-(1-hydroxyethyl)-2-methoxy-5-nitrophenoxy)-butanoic acid).

This material is available free of charge via the Internet at http://pubs.acs.org.

References and Notes

(1) Vernekar, V. N.; Cullen, D. K.; Fogleman, N.; Choi, Y.; Garcia, A. J.; Allen, M. G.; Brewer, G. J.; LaPlaca, M. C. *J. Biomed. Mater. Res., Part A* **2009**, *89A*, 138–151.
(2) Lin, C. C.; Anseth, K. S. *Pharm. Res.* **2009**, *26*, 631–643.
(3) Tibbitt, M. W.; Anseth, K. S. *Biotechnol. Bioeng.* **2009**, *103*, 655–663.
(4) Hahn, M. S.; Miller, J. S.; West, J. L. *Adv. Mater.* **2006**, *18*, 2679–+.
(5) Seidlits, S. K.; Schmidt, C. E.; Shear, J. B. *Adv. Funct. Mater.* **2009**, *19*, 1–9.
(6) Trenor, S. R.; Long, T. E.; Love, B. J. *Macromol. Chem. Phys.* **2004**, *205*, 715–723.
(7) Zheng, Y. J.; Mieie, M.; Mello, S. V.; Mabrouki, M.; Andreopoulos, F. M.; Konka, V.; Pham, S. M.; Leblanc, R. M. *Macromolecules* **2002**, *35*, 5228–5234.
(8) Fujiwara, T.; Iwata, T.; Kimura, Y. *J. Polym. Sci., Part A: Polym. Chem.* **2001**, *39*, 4249–4254.
(9) Iordanov, M. S.; Pribnow, D.; Magun, J. L.; Dinh, T. H.; Pearson, J. A.; Magun, B. E. *J. Biol. Chem.* **1998**, *273*, 15794–15803.
(10) Johnson, J. a.; Finn, M. G.; Koberstein, J. T.; Turro, N. J. *Macromolecules* **2007**, *40*, 3589–3598.
(11) Johnson, J. A.; Baskin, J. M.; Bertozzi, C. R.; Koberstein, J. T.; Turro, N. J. *Chem. Commun.* **2008**, 3064–3066.
(12) Kloxin, A. M.; Kasko, A. M.; Salinas, C. N.; Anseth, K. S. *Science* **2009**, *324*, 59–63.
(13) Kloxin, A.; Tibbett, M.; Kasko, A. M.; Fairbairn, J.; Anseth, K. S. *Adv. Mater.* **2010**, *22*, 61−66.
(14) Jay, S. M.; Saltzman, W. M. *Nat. Biotechnol.* **2009**, *27*, 543–544.
(15) Lutolf, M. P. *Nat. Mater.* **2009**, *8*, 451–453.
(16) Blow, N. *Nat. Methods* **2009**, *6*, 619–622.
(17) Aujard, I.; Benbrahim, C.; Gouget, M.; Ruel, O.; Baudin, J. B.; Neveu, P.; Jullien, L. *Chem.—Eur. J.* **2006**, *12*, 6865–6879.
(18) Furuta, T.; Wang, S. S. H.; Dantzker, J. L.; Dore, T. M.; Bybee, W. J.; Callaway, E. M.; Denk, W.; Tsien, R. Y. *Proc. Natl. Acad. Sci. U.S.A.* **1999**, *96*, 1193–1200.
(19) Zhao, Y. R.; Zheng, Q.; Dakin, K.; Xu, K.; Martinez, M. L.; Li, W. H. *J. Am. Chem. Soc.* **2004**, *126*, 4653–4663.
(20) Cruise, G. M.; Scharp, D. S.; Hubbell, J. A. *Biomaterials* **1998**, *19*, 1287–1294.
(21) Davies, H. G.; Wilkins, M. H. F.; Chayen, J.; La Cour, L. F. *Q. J. Microsc. Sci.* **1954**, *95*, 271–304.
(22) Reed, J.; Walczak, W. J.; Petzold, O. N.; Gimzewski, J. K. *Langmuir* **2009**, *25*, 36–9.